TEMPORAL CHARACTERISATION OF OPTICAL FREQUENCY COMBS

A Thesis

Presented to the Faculty of the Graduate School

of Cornell University

in Partial Fulfillment of the Requirements for the Degree of

Master of Science

by

Chaitanya Suhas Joshi

May 2013

ABSTRACT

The emerging field of silicon photonics allows us to develop more efficient networks that go beyond the capabilities and limitations of current electronic networks. Integrated photonic solutions in the present and in the future will allow us to keep pace with Moore's Law. Expertise in Silicon fabrication is at a very advanced level due to its use in semiconductor electronics. This expertise can be applied directly to fabricating optical devices using silicon as a medium of propagation for light. Silicon shows a high non linear optical response with high intensities. The high intensities required to see non linearity can be achieved by using waveguides etched into the silicon which confine light to a small mode area thus increasing intensity.

One application for silicon waveguide devices is the development of frequency combs. A frequency comb can act as an accurate frequency standard over a very large bandwidth that can range from the visible all the way through to the Mid IR. Applications for frequency combs can be found in high precision spectroscopy, optical metrology, highly precise optical atomic clocks and so on. By the very nature of its frequency spectrum, we expect to see short pulses in the temporal domain from a frequency comb. This thesis examines the building of an autocorrelation setup that can measure these pulses to high accuracy. We explore the choice of detection scheme, the choice of setup and go on to discuss some results from the setup that was built as part of the work leading up to this date.

BIOGRAPHICAL SKETCH

Chaitanya Suhas Joshi was born on Sunday the 3rd of September, 1989 in Thane, India. The eldest son of Meenakshi and Suhas, and the first grandchild of Snehalata and Laxman, he spent his first few days at home amid the festivities of the Ganesh Festival, and that is probably where his sweet tooth comes from. After completing various parts of his schooling in Pune, Clearwater FL, Trivandrum, Bangalore and back in Pune, Chaitanya completed his Senior Secondary Certificate from the Vikhe Patil Memorial School in Pune in 2005 with distinction. He went on to complete his Higher Secondary Certificate from the Modern College of Science in Pune in 2007 with distinction.

He matriculated the following Fall at the Indian Institute of Technology, Guwahati majoring in Engineering Physics. Among the various experiences that the institute gave him were a lifelong passion for swimming, classic rock and competitive quizzing. Academically, the institute enabled him to commence a process of learning in optics that has led eventually to this point in time.It enabled him to get a chance to visit TIFR in the summer of 2009 as an intern in the lab of Dr. Prabhu and at TU Delft in the summer of 2010 as an intern at the lab of Prof. Paul Urbach. These experiences also crystallised a resolve to go on to do graduate studies.

In the fall of 2011 he enrolled at Cornell University in the Master of Sciences program in Applied Physics. In his time on the hill he rediscovered his love for biking by exploring bike routes around Ithaca and Cayuga Lake. He worked on his thesis under the guidance of Prof. Alexander L. Gaeta exploring the temporal measurements of short pulses from a on chip frequency comb.

This document is dedicated to Aai Baba and Amol.

ACKNOWLEDGEMENTS

I would like to begin by thanking my advisor, Prof. Alexander L. Gaeta, who has been a great mentor over this past year. Over the course of our interaction I have come to find him as a very amiable and welcoming person to interact with and a brilliant teacher. At a crucial point of time when my work towards this thesis wasn't advancing as much as I would have been satisfied with, his input helped in kick-starting it and providing me with a much needed break.

I would also like to acknowledge Prof. Frank W. Wise for consenting to be on my committee and provide me with guidance if necessary. Although a significant part of my interaction with him has been outside the scope of this thesis, he has been very kind and approachable always.

I must also take this opportunity to thank various member of the Gaeta Group for their invaluable help, whether it be a major question about some part of my setup or something as simple as looking for a replacement for a blown fuse. Dr. Yoshi Okawachi for help and advice while I took baby steps on the project. Kasturi Saha for her guidance throughout the process of building the setup and for being ready to answer any question I had at any time. Sam Schrauth for his help on understanding autocorrelation when I started out and on ironing out many small issues as time went on. Dr. Stéphane Clemmen for his help on setting up the single photon APD. Alessandro Farsi for his help on the electronics and also for giving me a start on Python. I would also like to thank Hui Liu from the Wise group for her help on getting the autocorrelator working when it looked like there was no way to get it going.

And equally important to my being able to work effectively have been my friends here at Cornell and otherwise. They have been the best of buddies and the most effective support system that one could ever ask for. Ved and Shreyas,

Manchester United games had never been as much fun to watch as with you guys, and that twentieth title is going to be that much better for it. And you are the best housemates that one could ask for. Rohil, Avik, Sharvil, Pratham, Arjun, Kakat, JK, Ritika, Pranav the lunches, the coffees and in general a lot of exceedingly long random conversations are what keeps me going. Papps, Sharma, Kaali, Khabri, Golu, Ashay, Baccha, Max you always were and always will be the most amazing friends.

And last but not the least Aai, Baba thanks for the upbringing you have given me and all the opportunities you have made sure I get. Amol, the long talks about football and incessant bickering that we are almost always up to are, looking back, some of my best memories !

TABLE OF CONTENTS

LIST OF TABLES

LIST OF FIGURES

CHAPTER 1

INTRODUCTION

The higher we can go in terms of accuracy in the measurement of any standard unit takes us closer to the limits imposed on measurements by the uncertainty principle. Time (and interchangeably frequency) is a measurement, into the accuracy of which, a lot of work has been done over many centuries. We started off by measuring time using water clocks where our concept of time was based entirely on how much water had flown out of one container into the other, thus making the volume of one container the least count for accuracy in time. Then we went on to mechanical timepieces based on precisely crafted gears. Those bring down our accuracy to less than a second based on how precisely the gears are made. Optical Clocks go well beyond these accuracies by locking to the transition frequency between two well defined energy levels for an atom. Microwave optical clocks have demonstrated precision of the order of 10^{-16} locked to a microwave transition in Cesium atoms at GHz frequencies [1]. Moving to an optical frequency standard at THz frequencies can theoretically give us up to 10^5 better precision [2]. For this we need to have an optical source that has very well defined frequencies. A frequency comb is one such source of well defined frequencies of light [3].

Like the name implies, a frequency comb is an optical signal with a frequency spectrum consisting of a discrete series of ”comb” lines which are equally spaced. If we know the carrier envelope offset frequency and the comb spacing we can define each of the comb lines using just these two numbers and an integer. If a frequency comb has a bandwidth wide enough, it can act as a link between electronic and optical frequencies. We can create a ’custom’ opti-

cal signal using selected lines from the frequency comb, thus creating a optical signal generator using a frequency comb [3]. A series of discrete lines in the frequency domain leads to short pulses in the time domain. Very precise spectroscopy can also be done using a frequency comb [4]. Half of the Nobel Prize for 2005 was shared between Theodor Hansch and John Hall, for their work on spectroscopy using frequency combs. The pulse width is of the order of the inverse of the bandwidth, which means we can get down to femto-second range in pulse width. Pulses of the order of a few hundred attoseconds have been reported [5].

In Chapter 2 we discuss the frequency comb and some of the development seen in the past few years. We also discuss pulse measurement methodologies that were evaluated at the beginning of the work leading to this thesis. We chose to build an interferometric autocorrelation setup to measure these pulses. The theory behind interferometric autocorrelation is discussed in deeper detail. We also discuss Two Photon Absorption, as it is at the crux of our detection scheme for the setup.

In Chapter 3 we evaluate the performance of a normal silicon detector used in the setup. We make measurements for pulse width for a known fiber laser using this detector. We also study the two photon response to characterise this response for the detector. This detector worked well upto a certain lower limit of power, but we also consider a more sensitive detector to measure very low output power from the comb if this proves inadequate.

In Chapter 4 we evaluate a more sensitive detector. We used a silicon avalanche photo diode based single photon counter. We again take measurements that characterise the two photon response of the detector. We use this

detector to measure pulses at a lower powers than the limit on the normal detector. This serves as a proof of the ability of the setup to go down to power levels at which we expect the comb to be.

In Chapter 5 we discuss measurements made on the comb and the setup used for these measurements. An estimation of the expected power and pulse widths that we can expect from the comb is also made so as to compare it to the limitations of the respective methods.

CHAPTER 2

THEORY

2.1 Frequency Comb

A frequency comb can be completely defined by two frequencies, the carrier envelope offset frequency and the comb spacing. If we look at any periodic pulsed signal and apply a fourier transform, we will see a periodic signal in the spectral domain as well. The exact functional form of the spectral series varies with the functional form of the temporal pulses.

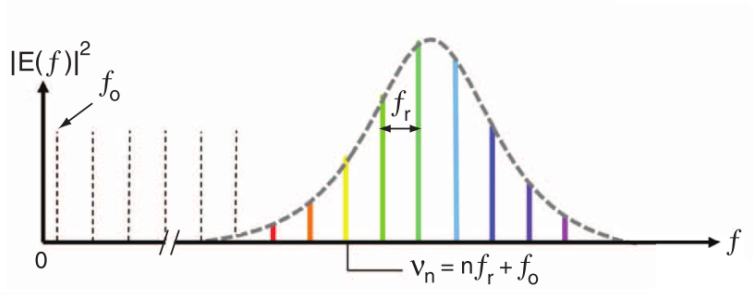

Figure 2.1: Power spectrum of a frequency comb.

The power spectrum of a typical frequency comb is as above in Figure 1 and consists of a series of comb lines that are completely defined by $f = f_o + m \times f_r$. f_r is the repetition rate of the cavity, whether it be a mode locked laser based comb or some of the newer platforms for frequency combs such as microrings, microtoroids etc. f_o is called the carrier envelope offset frequency. If we look at the temporal picture of these pulses, we can characterise it as a fast sinusoidal oscillation at the carrier frequency multiplied by a slower envelope [3, 6].

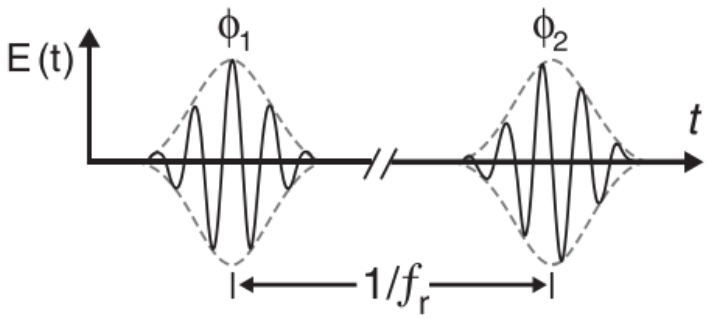

Figure 2.2: Temporal trace of pulses.

Here we can see that there is a shift in phase between the carrier sinusoid and the envelope. This shift is phase is given by $\Delta\phi = \phi_1 - \phi_2$. The separation between pulses is simply the round trip time for the cavity and hence, it is the inverse of the repetition frequency. The difference in phase $\Delta\phi$ between the envelope and carrier for successive pulses is a result of dispersion in the gain medium and non linear phase that the pulse picks up as it makes a round trip. The properties of the cavity and the gain medium are (usually) not time dependent. So the phase difference between successive pulses stays the same at $\Delta\phi$ the result of this carrier envelope phase offset is that the comb shifts by a fixed constant frequency i.e. the carrier envelope offset frequency f_o given by $f_o = \frac{1}{2\pi}\Delta\phi f_r$.[3]

If a comb is octave spanning, i.e. it has a bandwidth such that we have comb lines at frequencies f_m and f_{2m} we can determine the offset frequency by frequency doubling the lower comb line (using a SHG crystal) and looking at the beat frequency with the higher frequency comb line. $f_m = f_o + mf_r$ so $2f_m = 2f_o + 2mf_r$ and we have a comb line $f_{2m} = f_o + 2mf_r$ at the other end of the octave. The beat frequency when these two frequencies interfere is simply the offset frequency. This can be used as a feedback to stabilise the cavity and maintain the offset frequency at a specific value. That being said there are also

other methods to measure the offset frequency by using an known external frequency near one of the comb lines and looking at the beat frequency of that line with the comb line. However an octave spanning comb can be used in itself to find and stabilise the offset frequency [3].

The most common source of frequency combs has been Mode locking of Ti Sapphire lasers. A femtosecond laser based on a mode locked Ti:Sapphire laser was first reported in [7] with 60 fs pulses at a repetition rate of 75-100 MHz with a tunable cavity. Higher repetition rates mean wider spacing between comb lines. This is useful in precise frequency metrology which is one of the main advantages of frequency combs. To measure a frequency we measure its beat frequency (f_b) with the nearest comb line (f_m). Now this implies that the frequency to be measured is at $f = f_m \pm f_b$ so, to determine the frequency perfectly, we need to know a rough estimate of f using a standard spectrometer to within $f_r/2$ accuracy [3]. Higher repetition rates also mean more power in each individual comb line. The repetition rate is related to the cavity round trip time. Dispersion in a cavity results in broadening of the pulses as different frequency components see different delays. So a dispersion compensation mechanism has to be included in the Laser cavity while mode locking it. This adds to the cavity length and limits the maximum achievable repetition rate. By using improved optics such as low dispersion mirrors, or Gires-Tournois Interferometer Mirrors (which can give negative dispersion) the dispersion is managed without lengthening the cavity. However all of these do have a limit in terms of cavity length with the required dispersion management and gain medium (the Ti:sapphire crystal) all taking up space. To achieve a 1 GHz repetition rate we need a cavity that is 30cm in round trip length. 1 GHz combs have been reported in Ti:Sapphire mode locked lasers [8]. This is however close to the highest we can go on these solid state

platforms. Optical Fibers have been explored as a source for frequency combs, however these are limited to repetition rates of the order of around 100 MHz [9].Highly non linear fibers can be used to push cavity lengths to smaller values and increase the repetition rate in fiber based frequency combs. [6]

By going to much smaller cavity length scales, we can increase the repetition rate to the order of 100 GHz or even more. A 3 mm round trip cavity would give us a 100GHz comb. To realise such a small cavity we need to use microstructures that confine light to within these length scales. We use non linear optical processes in Whispering Gallery Mode microresonators to achieve the process of generation of a comb. Here light is confined to the perimeter of an interface by total internal refraction. Structures that support whispering gallery modes such as microtoroids [10], microspheres [11], CaF_2 WGM resonators [12] ring resonators on silicon [13] among others. These resonators are of the order of a few mm or a few cm in round trip length which give us higher repetition rates.

2.2 Pulse Measurement Techniques

In order to measure a periodic signal or for that matter a signal of any sort, we need a detector that has a measurement window that is shorter than that in width. The accuracy of our measurement is then limited to the width of the detector window. Ultra-short pulses that we generate from mode locked lasers and combs are among the shortest ever temporal signals that have been generated [14]. So measuring them is a challenge that requires a specialised setup. We know that a copy of the pulse is of the same width as itself which isn't a shorter reference and in most of the schemes that we discuss below we use this fact to

our advantage to create a measurement scheme.

Correlation is a measure of how similar two functions are for different values of the independent variable. Mathematically speaking the correlation of two functions is given by.

$$(a \star b)(t) = \int_{-\infty}^{\infty} a * (\tau) b(t + \tau) d\tau \tag{2.1}$$

where a* is simply the complex conjugate of the function A. If we look at this integral, we introduce a time delay of τ in one of the functions and integrate over all values of this delay. If $a(t) = b(t)$ we are simply measuring the similarity of a function with a time delayed copy of itself. This is the Autocorrelation function for $a(t)$.

2.2.1 Intensity Autocorrelation

In an optical autocorrelation, we measure the similarity of a pulse with itself. This gives us some insight into the variation of Phase and Intensity of a pulse with time. A laser pulse has a time domain field given by,

$$E(t) = Re[I(t)^{1/2} e^{i\omega_0 t - i\phi(t)}] \tag{2.2}$$

Where $I(t)$ and $\phi(t)$ are respectively the temporal Intensity and Phase functions. Optical Autocorrelations as a method for characterising optical pulses have been around for about half a century now, being first reported in 1966-67 [15, 16]. Typical detectors that we use have rise and fall times of the order of 1ns due to limitations in the associated electronics that let it go only upto the order of a few GHz at the most. So any pulse that is shorter than ~1ns needs a specialised detection scheme. [17]

To measure the variation of intensity of the pulse with time we split the pulse into two parts and send them through two different delays one a fixed delay and the other a variable delay. In this way we create a variable spatial separation between the two pulses. We then overlap these two pulses in a Non linear optical medium such as a second harmonic generation crystal. The SHG crystal will produce light that is at a frequency twice that of the input light with a field given by. [18]

$$E_{SHG} \propto E(t)E(t-\tau) \tag{2.3}$$

Where τ is the delay we introduce in one of the copies of the pulse. Since the Intensity is given simply by $2cn\varepsilon_0|E|^2$ the intensity of the second harmonic signal is proportional to the intensities of each of the pulses.

$$I_{SHG} \propto I(t)I(t-\tau) \tag{2.4}$$

Note here that only the cross term for the two pulses appears because we selectively measure the second harmonic light that is emitted along the optical axis. There are other components at different angles that we don't measure. If we introduce a path delay of 1 μm for one of the pulses, the temporal delay that it corresponds to is 3.33 fs. In this way we create a variable temporal delay in between the two pulses and see a corresponding variation in the second harmonic signal. Since detectors are slower than the time scales they aren't able to resolve this signal in time. The signal that the detector measures is given by

$$A^{(2)}(\tau) = \int_{-\infty}^{\infty} I(t)I(t-\tau)dt \tag{2.5}$$

This is just the autocorrelation function of the intensity which is what we started out trying to measure. Note that this is a function of the delay and not actual time. We can slow down the variable delay to larger time scales because we are creating the temporal delay using a spatial path difference.[17]

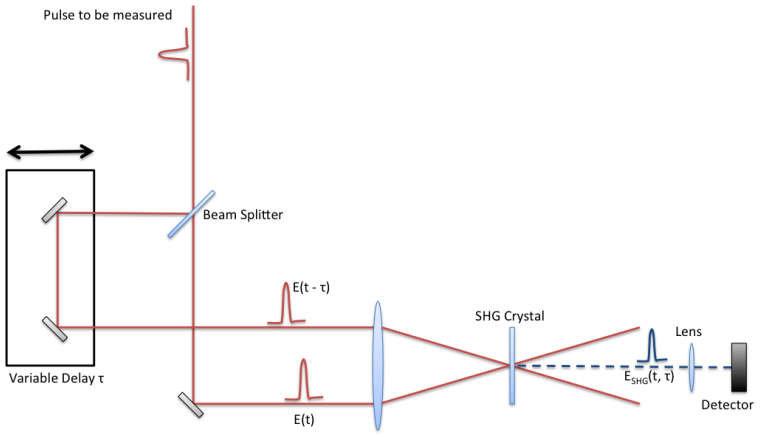

Figure 2.3: Schematic of a setup for an intensity autocorrelation.

The relationship between the FWHM of the autocorrelation trace and that of the Pulse is dependant on the shape of the pulse [19]. This relationship is as given in Table 2.1

Pulse Shape	I(t)	$A^{(2)}(\tau)$	τ_{AC}/τ_p
Square Pulse	$1; \lvert t\rvert \leq \tau_p/2$ $0; \lvert t\rvert \geq \tau_p/2$	$1 - \lvert\frac{\tau}{\tau_{AC}}\rvert; \lvert t\rvert \leq \tau_{AC}$ $0; \lvert t\rvert \geq \tau_{AC}$	1
Gaussian	$e^{-[\frac{2\sqrt{ln2}t}{\tau p}]^2}$	$e^{-[\frac{2\sqrt{ln2}t}{\tau_{AC}}]^2}$	1.41
$sech^2$	$sech^2[\frac{1.7627t}{\tau_p}]$	$\frac{3}{sinh[\frac{2.7196\tau}{\tau_{AC}}]}[\frac{2.7196\tau}{\tau_{AC}} coth[\frac{2.7196\tau}{\tau_{AC}}] - 1]$	1.54

Table 2.1: Pulse shapes, pulse widths, autocorrelation trace widths for different pulse shapes

There is a fair amount of uncertainty when measuring a pulse simply based on its intensity autocorrelation. Many different temporal intensity profiles yeild very similar autocorrelation traces. So we usually assume a pulse shape and calculate the pulse width from the width of the autocorrelation trace. Typically

for ideal ultrafast sources we get a theoretical sech^2 solution so it is chosen as the pulse shape most commonly.

2.2.2 Interferometric Autocorrelation

In the intensity autocorrelation, by sending in the two copies of the pulse at an angle, we ensured that we measure only the cross term (eqn. 2.3). However if we align the pulses co-linearly along the optical axis and send them through a SHG crystal then we get some more terms in the measured trace. The electric field incident on the SHG crystal is given by,

$$E_{inc}(t) = E(t) + E(t-\tau) \tag{2.6}$$

Consequently the Second Harmonic Crystal will double the frequency and the detector will measure the intensity integrated over time.

$$IAC(\tau) = \int_{-\infty}^{\infty} |[E(t) + E(t-\tau)]^2|^2 dt \tag{2.7}$$

$$= \int_{-\infty}^{\infty} |E(t)^2 + 2E(t)E(t-\tau) + E(t-\tau)^2|^2 dt \tag{2.8}$$

As mentioned above, the co-linear propagation adds the second harmonic terms from each individual pulse and also their interference with each other and the cross term. We filter out light at the fundamental frequency and only keep the light at the doubled frequency which eliminates terms like $I(t)$ and $I(t-\tau)$ and the interference term $E(t)E(t-\tau)$.

If we look more closely at what the detector measures, expanding Eqn 2.8 we can separate the Interferometric Autocorrelation into 4 separate terms each with

their own information about the pulse.

$$\begin{aligned} IAC(\tau) = & \int_{-\infty}^{\infty} I^2(t) + I^2(t-\tau)dt \\ & + 4\int_{-\infty}^{\infty} I(t)I(t-\tau)dt \\ & + 2\int_{-\infty}^{\infty} [I(t) + I(t-\tau)]E(t)E^*(t-\tau)dt + c.c \\ & + \int_{-\infty}^{\infty} E^2(t)E^{2*}(t-\tau)dt + c.c \end{aligned} \tag{2.9}$$

Here the first term is simply the Square of the intensities of the two individual pulses. This is the same irrespective of delay. The second term is the Intensity Autocorrelation. The third term is a Field Interference term weighted by the sum of intensities. The fourth is a interference term between the second harmonics generated. The third and fourth terms lead to fringes in the measured autocorrelation.

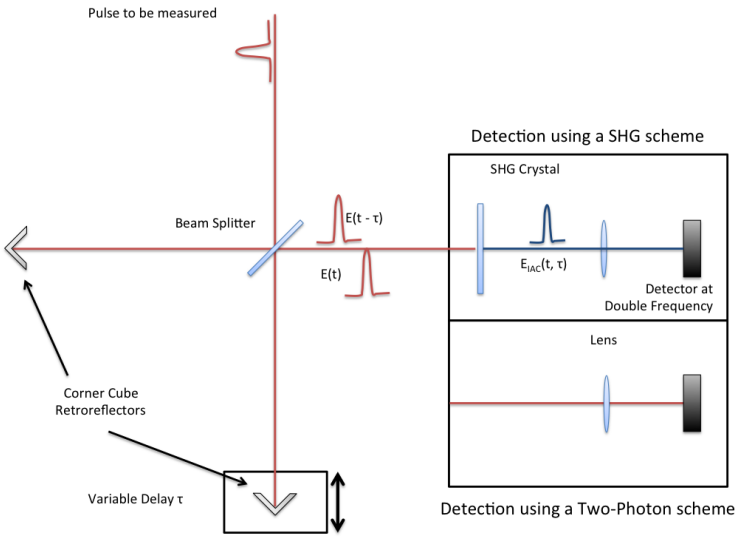

Figure 2.4: Schematic of a setup for an interferometric autocorrelation.

2.3 Two Photon Absorption

We chose to use the Interferometric Autocorrelation with Two Photon absorption as a detection scheme. A Two Photon absorption event can occur over a wide band of frequencies based on the very simple requirement that the energy be more than half of the band gap of the detector material and less than the bandgap itself. There are several other factors that will also affect the probability of two coincident photons being absorbed, that will reduce the bandwidth over which Two Photon absorption occurs, however as the upper limit of Two Photon absorption bandwidth this simple assumption works. If we perform a rough calculation based on published values of Silicon bandgap in any common Solid State textbook (1.12 eV) we can see that Two Photon Absorption is possible at any wavelength corresponding to energies such that.

$$\frac{E_g}{2} \leq E_\lambda < E_g \tag{2.10}$$

These, in the case of bulk silicon (which is an assumption we make for the silicon detector surface) would correspond to

$$1107 \text{ nm} \leq \lambda < 2217 \text{ nm} \tag{2.11}$$

This covers an appropriate section of the spectrum within which most if not all of our comb lines should lie. One more advantage of the use of the TPA detection is phase matching in the SHG crystal for the other option of setup. Phase matching is an extremely important part of generating Second Harmonic frequencies. The required conditions have been discussed at great length in [18]. In addition, the phase matching conditions may be valid for a section of the comb, but may not be valid for every comb line. This would hinder our ultimate aim of measuring pulses by sending in the entire comb. To observe a two

photon event, the only requirement is that the photons arrive at the detector simultaneously. This can be at any wavelength provided it falls within the limist as stated in Eqn. 2.10.

Two Photon absorption was predicted by Maria Göppert-Mayer, who went on to win a Nobel Prize in Physics for her work on proposing the nuclear shell model, in her doctoral thesis. We can look at Two-Photon absorption in two ways, one being the quantum mechanical picture, the other being Two Photon absorption as a consequence of the imaginary part of the third order non linear susceptibility in a material.

2.3.1 Quantum Mechanical Explanation

If we look at the band gap structure of any material, there are two energy levels, the valence and conduction bands, which are separated by the band gap energy. If a single photon with an energy less than the band gap is incident, we will not see any absorption. If a photon with an energy greater than or equal to the band gap is incident, we see linear absorption. If two photons with more than half the band gap energy but less than the band gap energy itself are simultaneously incident on the detector, there is a finite probability of them being absorbed. 'Simultaneity' in this process is defined in terms of a virtual intermediate level (denoted by the dashed line in Fig. 2.5.) the 'first' photon undergoes a transition to this virtual level. If the 'second' photon is incident within a time delay equal to the virtual lifetime of this level the transition from the Valence to the conduction band is achieved. This is just a qualitative idea of the process behind Two Photon absorption. A complete mathematical study of the theory of multipho-

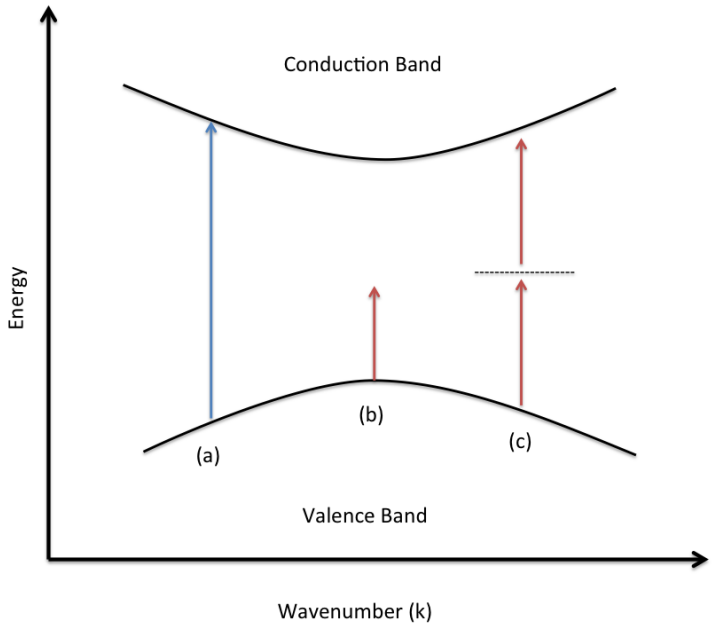

Figure 2.5: Transitions in a material with a finite band gap (a) linear absorption (b) no absorption (c) two photon absorption.

ton absorption using quantum mechanics is given in [18] where they show the rate of Two-Photon absorption is proportional to the square of the Intensity of incident light.

2.3.2 Third Order Non-Linear Susceptibility

For a non linear optical material the polarisation is dependent on the Electric field non linearly. The polarisation is given by

$$\vec{P} = \varepsilon_0 \chi^{(1)} \vec{E} + \varepsilon_0 \chi^{(2)} \vec{E}^2 + \varepsilon_0 \chi^{(3)} \vec{E}^3 + ... \tag{2.12}$$

Two photon absorption can be explained by the imaginary part of the $\chi^{(3)}$ term. If we look at an inversion symmetric medium (which is true for all but a few optical materials) the even order terms in Eqn. 2.12 drop to zero due to this

symmetry. If we look at the third order term in the polarisation as a function of frequency closely and split it component-wise axially we have,

$$P_i^{(3)}(\omega = \omega_1 + \omega_2 + \omega_3) = \varepsilon_0 D^{(3)} \sum_{jkl} \chi_{ijkl}^{(3)} E_j(\omega_1) E_k(\omega_2) E_l(\omega_3) \tag{2.13}$$

The $D^{(3)}$ is the degeneracy factor associated with the permutations of the three frequencies in the polarisation term. For the case of two photon absorption the degeneracy is 3. $\omega_1 = \omega_2 = -\omega_3$ and the two other permutations of frequency. Now if we want to consider the propagation of light in this medium we need to use the non linear wave equation. The general form of the wave equation is a direct result of the Maxwell's Equations and is given by.

$$\nabla \times \nabla \times \vec{E} + \mu_0 \frac{\partial^2 \vec{D}}{\partial t^2} = 0 \tag{2.14}$$

Plugging in the non linear $\vec{P}$ into the expression for $\vec{D}$ we get a form of the wave equation incorporating the non linear polarisation term.

$$-\nabla^2 \vec{E}(r,t) + \frac{n^2}{c^2} \frac{\partial^2 E(r,t)}{\partial t^2} = -\mu_0 \frac{\partial^2 P^{NL}(r,t)}{\partial t^2} \tag{2.15}$$

Assuming sinusoidal fields we can rewrite it as

$$-\nabla^2 \vec{E}(r,\omega) + \frac{n^2 \omega^2}{c^2} \vec{E}(r,\omega) = -\mu_0 \omega^2 \vec{P}^{NL}(r,\omega) \tag{2.16}$$

In a simplified system with an isotropic medium and a field polarised along the x axis and the direction of propagation along z this becomes,

$$\frac{\partial^2 E_x(z)}{\partial z^2} + \frac{n^2 \omega^2}{c^2} E_x(z) = -3 \frac{\omega^2}{c^2} \chi_{xxxx}^{(3)} |E_x(z)|^2 E_x(z) \tag{2.17}$$

Further with the slowly varying envelope assumption we get

$$\frac{dA(z)}{dz} = \iota \frac{3\omega}{2nc} \chi_{xxxx}^{(3)} |A(z)|^2 A(z) \tag{2.18}$$

χ_3 is imaginary and hence it leads to real and imaginary terms in $\frac{dA(z)}{dz}$. The real part of $\frac{dA(z)}{dz}$ leads to the intensity dependent TPA and the imaginary part leads

to the intensity dependant refractive index. This gives us the TPA coefficient as,

$$\beta = \frac{1}{I^2}\frac{dI}{dz} = \frac{3\omega}{2\epsilon_0 nc}\mathrm{Im}(\chi^{(3)}_{xxxx}) \tag{2.19}$$

This shows us the I^2 dependence of the absorption of photons. In our two photon absorption based autocorrelation setup, we use this fact to measure the overlap of two pulses with a delay in between them. The intensity varies as the delay varies and this in turn changes the two photon absorption photocurrent that we see. This can be used in the characterisation of the pulses by the autocorrelation methods we have described above [20].

CHAPTER 3

NORMAL SILICON DETECTOR CHARACTERISATION AND RESULTS

We present some results from a normal silicon photodiode used in our autocorrelation. This photodiode has some limitations with respect to the power it can go down to. This limit is also discussed.

3.1 Detector Properties

We characterize and present some results from our setup using a normal silicon photodiode. The photodiode (Hamamatsu S-1223-01) was used in the autocorrelation setup. We used this photodiode to measure the overlap as a function of delay, that is the autocorrelation trace. The linear sensitivity curve for the photodiode is as given in Fig 3.1. This curve indicates that at 1550nm, which is

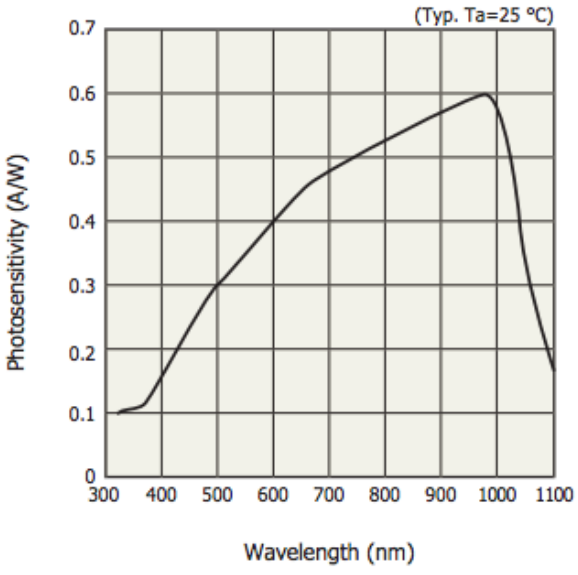

Figure 3.1: Spectral response curve for the Hamamatsu S-1223-01 photodiode at room temperature.

at about the center of the comb frequencies that we will be sending into the autocorrelator, the detector has a very low linear response. Since the two photon response is related to the intensity of light incident upon it, we focus down on the detector using an aspheric lens (Newport 5721-H-A) with a focal length of 2.8mm.

The detector was characterised using a CW source to investigate if it shows a Two-Photon response as expected. We plot the measured photocurrent as a function of average incident power. This plot shows an initial rising trend

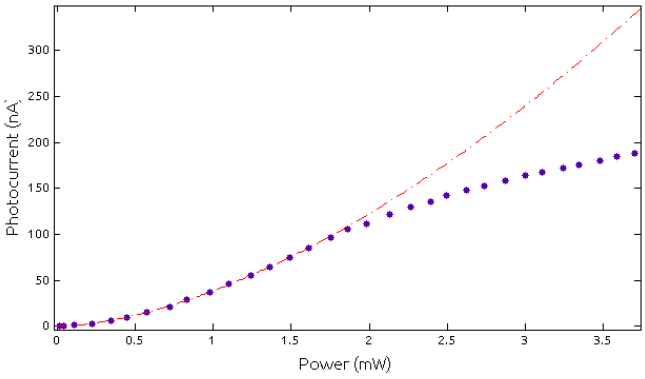

Figure 3.2: Two photon response characterisation curve for normal Silicon detector.

and then seems to level off. We suspect that this is due to detector saturation at higher powers. When fit to a functional form $a * x^b$ we get b = 1.669. For a purely two photon process we would have expected to see b = 2, however 1.669 seems to indicate that there is also some amount of linear absorption in the detector, albeit fairly low as compared to the two photon.

3.2 Fiber Laser and Fiber Amplifier

To test the autocorrelator and check how low we can go in terms of average power, we use a fiber laser with a fiber amplifier. The fiber amplifier is used if needed to ramp up the power. The laser properties (unamplified) are as given in Table 3.1

Laser Repetition Rate	38 MHz
Laser Peak Wavelength	≈ 1570 nm
Laser 3dB Bandwidth	≈ 4-5 nm

Table 3.1: Fiber Laser Characteristics

We use the laser as an input to the amplifier, vary the amplifier current and measure the average power from the output. The average power varies linearly with the amplifier current. This is useful as is gives us a way to vary power while testing the detector without introducing an additional non linearity.

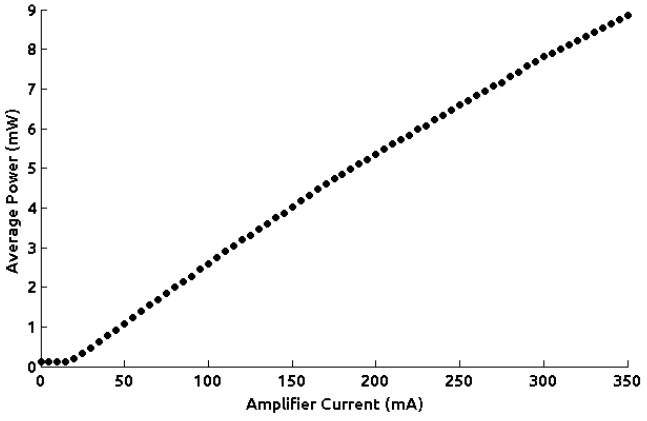

Figure 3.3: Fiber amplifier characterisation.

3.3 Setup

The setup we chose to build is an Interferometric Autocorrelation setup. We couple light in through a fiber collimator. We guide the beam through a set of mirrors to a pellicle beam splitter. The pellicle splits in the ratio of approximately 45:55 R:T at the wavelength range we are interested in. The transmitted beam goes onto a Gold Corner Cube Retroreflector mounted on a translation stage that is used to accurately position the mirror on this arm so that . The reflected beam goes to another Gold Corner Cube Retroreflector that is mounted on a electromagnetic shaker. The shaker is driven by a triangular signal from a signal generator. These two beams are recombined and focussed down onto the detector by an aspheric lens.

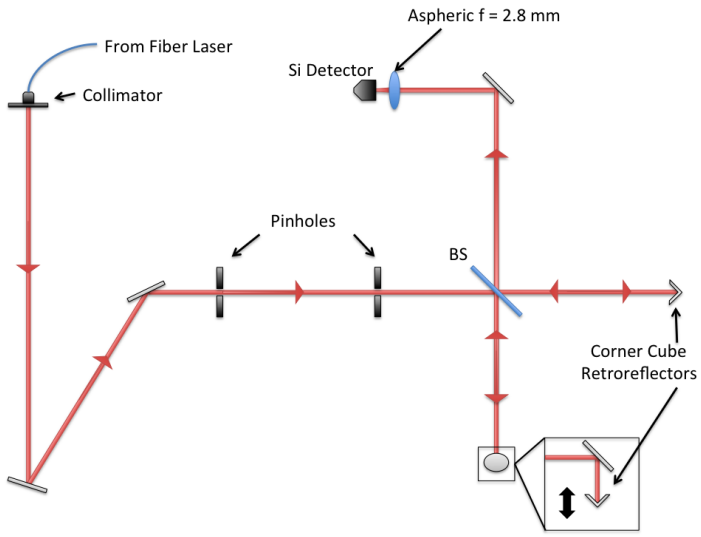

Figure 3.4: A schematic of the setup used to measure traces from the fiber laser using the normal detector.

3.4 Results

We present some of the results from the setup using a normal detector. Initially the shaker was being driven at 20 Hz. As it turns out, at this speed of oscillation, the fringes in the interferometric autocorrelation get averaged out and we measure only the background constant term and the Intensity Autocorrelation (i.e. the first two terms from Eqn. 2.9). We measured using this detector a pulse with some amplification. The shaker rate is 20Hz, the width of the measured

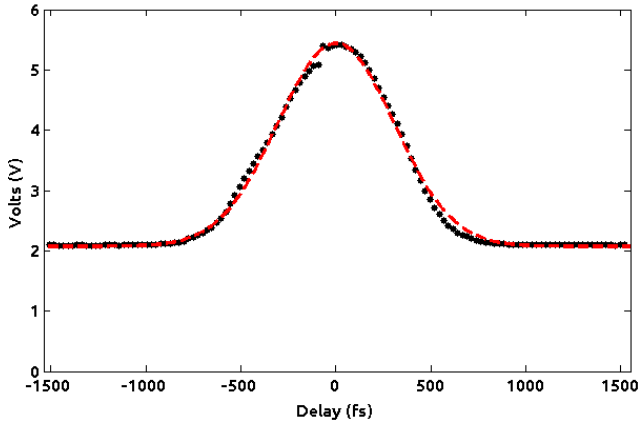

Figure 3.5: A measured autocorrelation trace using the normal detector.

autocorrelation trace is 718 fs. Assuming an ideal sech^2 pulse at the laser output this comes out to be a pulse width of 467 fs. The The average power measured is ~ 5.75 mW. The pulse energy is calculated to be ~150 pJ based on the average power measured and a repetition rate of 38 MHz for the laser. This measurement was performed with the fiber amplifier set to a current of 100mA.

We expect the contrast ratio for the trace in Fig. 3.5 to be 3:1 whereas we have a contrast of ~ 5.5:2.1. We investigated the source of this anomaly, and discovered that the power going onto the detector from both arms wasn't exactly 50:50. The

cause for this was an additional mirror in one of the arms that was introducing a loss. The design of the setup is such that that particular mirror was indispensible so we had no choice but to keep things the way they were. As a precaution we replaced that mirror with a broadband mirror with as high a reflectivity as we had.

At amplifications lower than this value and at 20Hz we were still able to see a autocorrelation trace, however, calibration for this trace becomes fairly unreliable. Some calculations for the power we expect to see from the comb are given in a later section. Based on this it seems that we need a more sensitive detector. This detector is discussed in the next chapter.

Later on while trying to look at traces from a wider bandwidth fiber laser (implying a shorter pulse duration) we realised that driving it slower with a narrow amplitude not only allows us to see the fringes, but also, since the integration time on the detector is higher, allows us to go to lower powers. We measure the traces from a fiber laser with a wider bandwidth (and consequently lower pulse widths) with the same repetition rate of 38 MHz as before.

CHAPTER 4

SINGLE PHOTON COUNTING MODULE CHARACTERISATION AND RESULTS

Based on the limitations on power that the normal detector imposed upon us we decided to go for a more sensitive used in our autocorrelation. The choice of detector was prompted in part by the use of a similar detector in [21].

4.1 Detector Properties

We use a Perkin Elmer SPCM-AQR-16 single photon counter which is just a silicon detector working in the Geiger mode(i.e. The reverse bias voltage applied to the device is above the breakdown level). We again characterise the detector using a variably amplified source and see if the photon counts follow a quadratic rise with incident power. We couple light into a fiber and then through a 70:30 splitter we send the 30 to a power meter and the 70 is coupled to the detector using the fiber coupling mechanism on the detector. The fiber coupling option is attached onto the detector using screws so the alignment is quite poor. We expect that better alignment could have been achieved with free space coupling, but at the risk of damaging the detector, so we refrained from a free space coupling setup immediately. The photon counts rise with a very noticeable quadratic trend. A quadratic has been fit to the curve in Fig 4.1. The fiber coupling to the detector was sub optimal, so we expect that the power actually incident on the detector is lower than we have measured using the 30 portion of the 70:30 split.

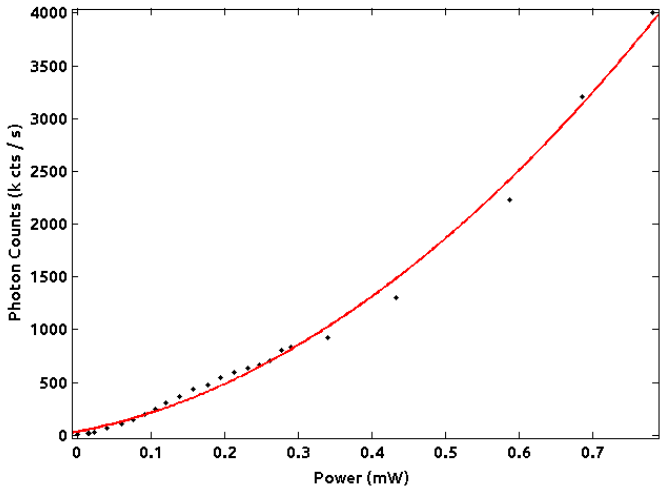

Figure 4.1: Two photon response characterisation curve for the single photon counting module.

The characterisation was done on a detector that has a minimum counting interval of 0.01s (BK Precision 1823-A) Since we were using the shaker at 20Hz this wasn't going to be enough resolution to measure traces. We changed to a faster counter (NI BNC-2121).

4.2 Setup

The setup is almost identical to the setup for the normal detector with the small change that we add a periscope at the end to get the beam height down to the level of the detector. The same initial path is used as before through the 45:55 pellicle beamsplitter and reflected off corner cube retroreflectors and recombined onto the periscope.

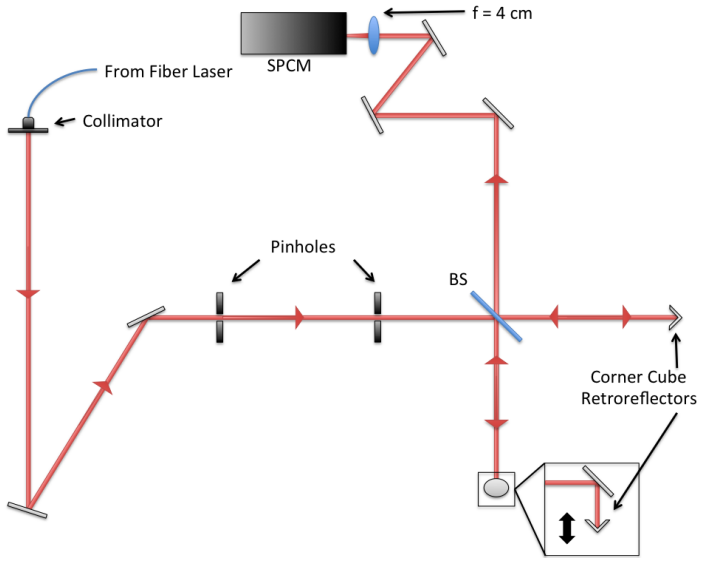

Figure 4.2: A schematic of the setup used to measure traces from the fiber laser using the single photon detector.

4.3 Results

We present some of the results from the measurements using the single photon detector. Due to the increased sensitivity we did not need to use an amplifier. We are able to measure directly from the fiber laser without any major issues. The single photon detector counts have a lot of noise and hence there is a need for a lot of averaging. Here again we drive the shaker at 20Hz resulting in the fringes being washed out by averaging. A direct trace of the autocorrelation is given in Fig. 4.3. We see clearly that the signal is fairly noisy. To improve this we considered both active smoothing, wherein we applied a Gaussian Moving Average filter over the data set while acquiring, however the problem with this was that this amounts to convolution with a Gaussian of a certain width. Convolution of two Gaussians results in a wider signal and this would affect our calibration, so we decided to take data over a long time and then average over the individual traces. This way the measured signal width isn't affected.

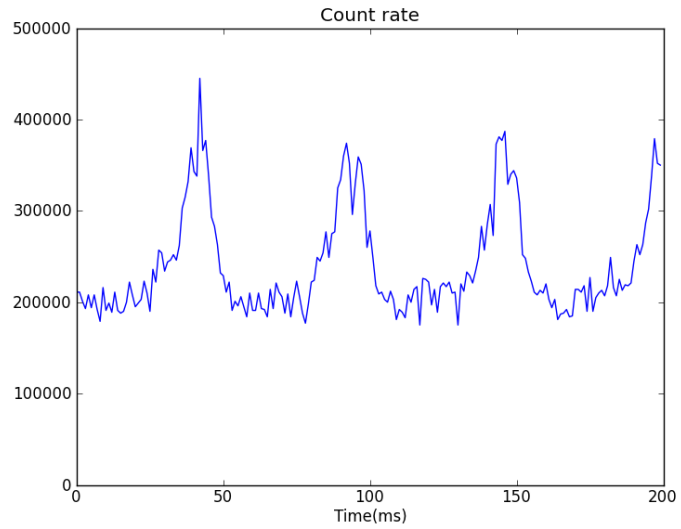

Figure 4.3: Direct trace of the autocorrelation using the SPCM.

To smooth out the traces we measure a large number of traces without chang-

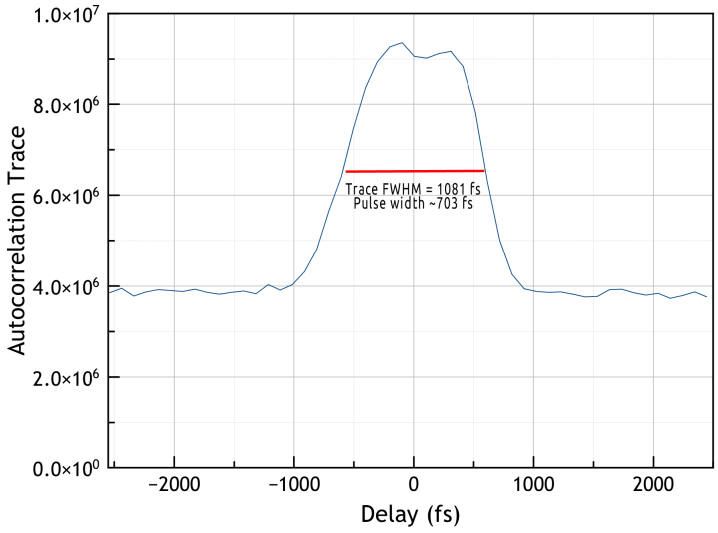

Figure 4.4: Autocorrelation trace using the SPCM from a 10s dataset.

ing the setup so as to get enough data to allow for smooth averaging. A trace taken for 10 seconds with averaging is given in Fig. 4.4. The dip noticeable at

near zero delay is just an artefact of the noisy nature of the signal.

To verify the measurements from the fiber laser, we compare results when we send the full fiber laser output through and then with a WDM filter out a section and send that through. We would expect to see wider pulses with the filtered section of the fiber laser and that would serve as verification that the autocorrelator is working as expected. The spectra and measured traces are presented below. The measured traces do show the expected widening as we

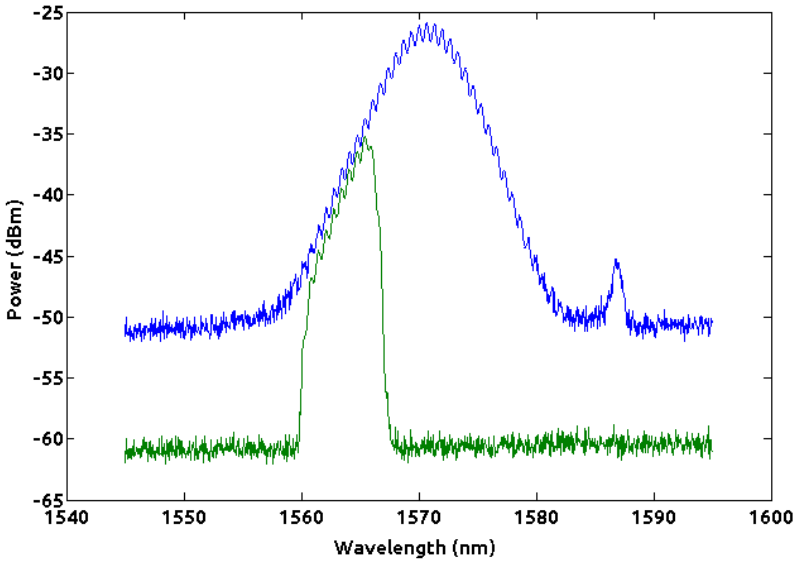

Figure 4.5: Spectra of the fiber laser with (green) and without (blue) the WDM.

shorten the bandwidth. The traces with and without the WDM are given below in Fig 4.6. and 4.7. We see Autocorrelation trace width of 1211 fs corresponding to a pulse width of 787 fs in the trace without the WDM. For the case of the pulse with the WDM, we see a wider Trace FWHM of 1863 fs corresponding to a pulse FWHM of 1210 fs. This seems to indicate that the autocorrelator is working as expected.

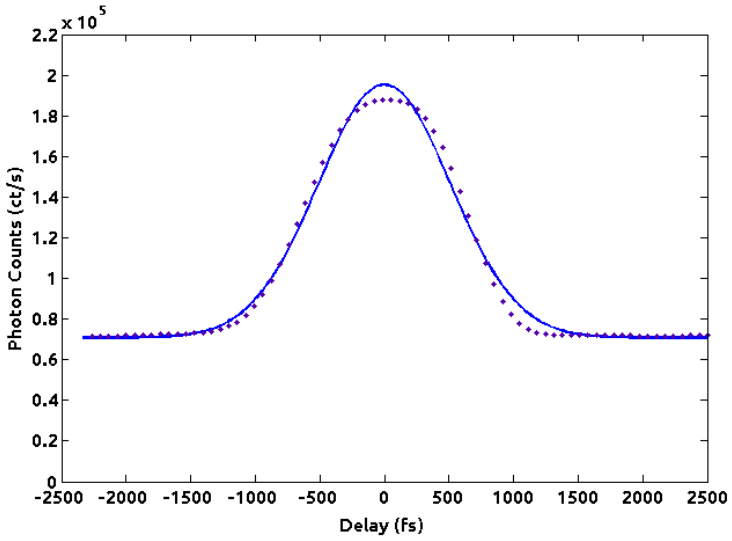

Figure 4.6: Autocorrelation trace and gaussian fit without the WDM.

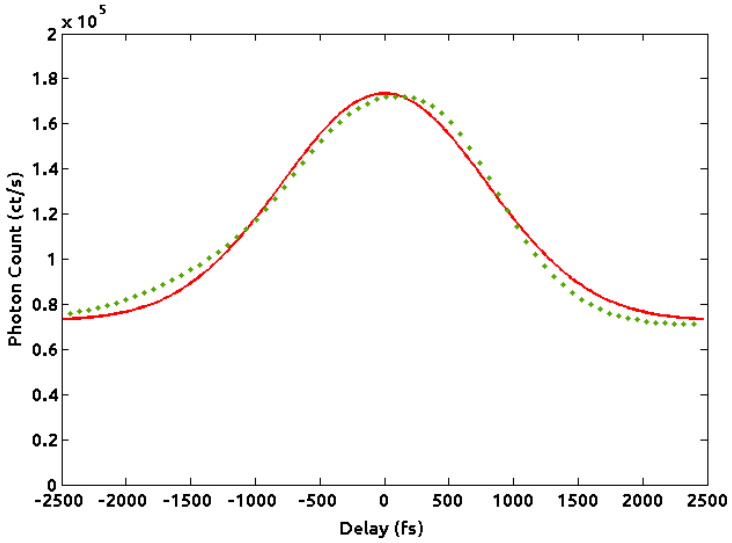

Figure 4.7: Autocorrelation trace and gaussian fit with the WDM.

The power level on the fiber laser was high enough to give us adequately good results. We then went on to attenuate the fiber laser using a variable OD filter wheel and measure pulses. We were able to go down as far as 20μW of average power from the 38MHz laser. This corresponds to $\sim$ 530 fJ which is 3 orders of magnitude better than the limit on the normal detector. After getting these

results we decided to take the setup to the comb setup and send light from the comb into the autocorrelator to measure pulse widths on the comb.

CHAPTER 5

FREQUENCY COMB MEASUREMENTS AND RESULTS

5.1 Properties of the Frequency Comb

The frequency comb that we are using is a 200GHz repetition rate comb pumped at about 1560 nm using a CW source. One thing that we can see from this spec-

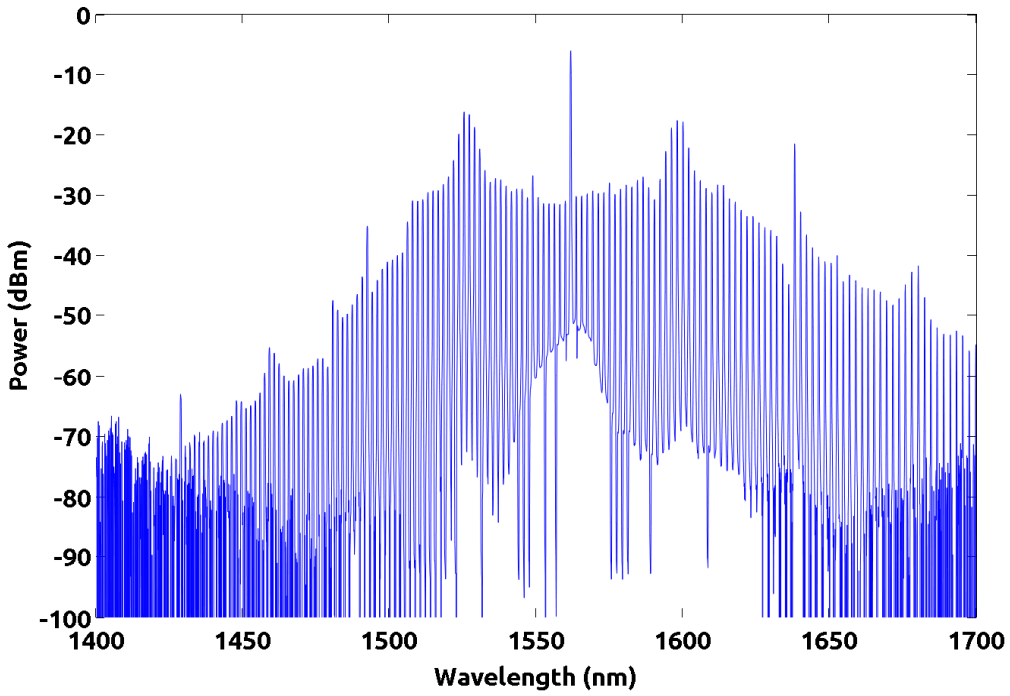

Figure 5.1: Spectrum of the 200 GHz comb with a pump at 1560 nm.

trum is that most of the pump goes through the chip and we see a fairly high line at the comb wavelength that is at least 10-12 dBm higher than any of the other comb lines. If we directly send the comb through, this strong pump line is probably going to lead to a very strong DC on which small pulses are superimposed. There is a high chance that the small pulses are going to be lost

completely in the noise. So, filtering out the pump or attenuating it becomes a necessity.

5.2 Comb Power Calculations

We assume a fairly pessimistic average 100 μW per comb line to estimate the power from the comb. The pump is at around 1560nm. We calculate our expected power and pulse width for a 100nm band centered around the pump (1510-1610nm) with the assumed power per comb line. We also assume a sech^2 pulse shape and transform limited pulses.

Central Wavelength = 1560 nm

Bandwidth = 100 nm

Pulse Repetition Rate = 200 GHz

Power per Comb Line = 100μW

Bandwidth (100 nm @ 1560 nm) = 12.34 THz

Transform Limited Pulse Width = 0.32 / Bandwidth = 25.9 fs

Number of Comb Lines ~ 61

Average Power = 6.1 mW

Pulse Energy = 30.5 fJ

Peak Power = 1.17 W

5.3 4-f Shaper

To filter out the pump singularly, we need a very narrow notch filter. Achieving this using a WDM is possible. However rather than finding a very narrow WDM ($\leq$ 2 nm) at exactly the pump wavelength, it is easier to use a 4-f shaper which we discuss below.

A 4-f shaper is based on the spatial separation of frequencies when reflected off a grating (1st order reflection) we then selectively attenuate the frequencies that we want to remove or modify. This is achieved by means of a spatial block / attenuator. A 4-f shaper consists of a grating and a lens from which the light is decomposed into its spectral components. At the focal plane of the lens we place our filtering mechanism. The focal plane of a lens is also the Fourier Transform plane. This comes as a direct consequence of the Diffraction integral [22]. The spectral components, modified by the filter placed at the Fourier plane are then recombined by another lens onto another grating which recombines the spectral components into a single beam. The returning beam has the spectrum of the original pulse multiplied by the filter placed at the Fourier transform plane. The name 4-f simply refers to the distances between the components. The grating and lens are seperated by f, the two lenses are separated by 2f and the second lens and grating are a further f apart, where f is the focal length of the lenses.

The setup can be built using two lenses and gratings or with a single lens and grating. The two lens,two grating setup is called a one pass 4-f shaper. The single lens, single grating one is called a double pass 4-f shaper. If we put the filter and a mirror at the focal plane and reverse the path, the lens acts as the

second lens and the grating as the second grating. We built a 4-f shaper with a mirror, i.e. a double pass 4-f shaper with a needle blocking out the filter. The needle is placed slightly ahead of the mirror which is exactly aligned to the focal plane. The needle filters out a 4nm span from the spectrum around the pump wavelength. This can be reduced further if needed by moving the needle closer to the mirror.

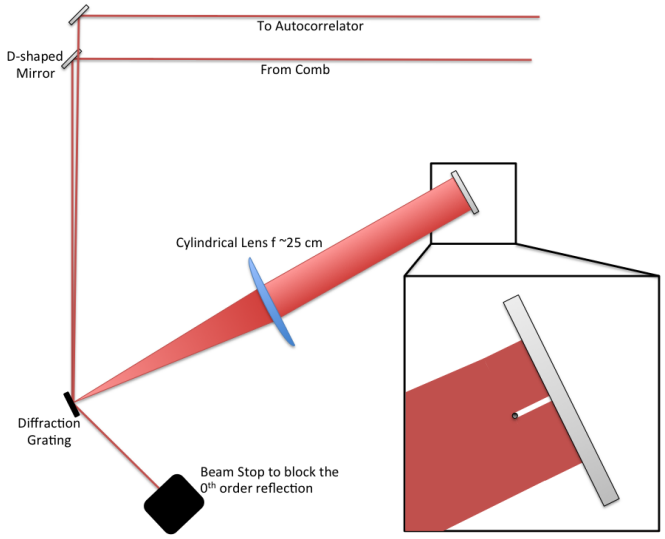

Figure 5.2: Schematic of the 4-f shaper setup used.

5.4 Comb Measurements

We send the generated comb through the 4-f shaper which filters out the high pump level. In this way we aim to prevent the pulses from the comb from being small in amplitude as compared to the CW from the pump that passes through the chip. We expect to maintain pulse shape when it returns from the 4-f shaper, however in our setup we see an elongation of the beam along a direction paral-

lel to the grating lines. This is something we haven't been able to explain with a lot of confidence yet. To gather all the light from this elongated beam, we put in a telescope using cylindrical lenses so that we can reduce the size in that dimension. A schematic of the telescope is given in Fig. 5.3. However chromatic

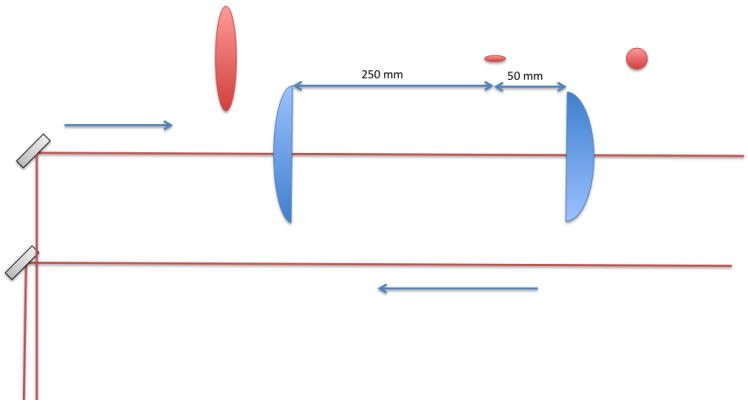

Figure 5.3: Schematic of the telescope used to shape the beam.

aberrations in the cylindrical lenses seem to be preventing us from optimising the telescope. We can accurately collimate the beam for a single wavelength (say the pump wavelength) but as soon as we send the entire comb in we begin to see natural diffraction of the beam after passing through the telescope.

The elongated shape of the beam means that when we try to focus down onto either of the detectors we get suboptimal focussing. The fact that we are unable to get all the power to the detector prevents us from seeing enough two-photon absorption to see the pulses from the comb. However even with the suboptimal focussing we still are able to see a two photon response. This is indicative of the fact that we should potentially be able to see a lot more two-photon response if

we can gather all the light properly.

5.5 Future Course of Work

The future course of work will be to identify the source of this elongation and if possible to correct this elongation of the beam before focussing it down onto the detector. If the elongation is the result of a natural diffraction, then we would want to make the telescope better so that we can collect more of the beam onto the detector. If we are able to gather all the power from the comb onto the detector, the calculations indicate that we should be able to measure the pulses to good accuracy.

APPENDIX A

DEVICES USED IN THE EXPERIMENTS

A.1 Detectors

Hamamatsu S-1223-01 - Normal Si PIN Photodiode

Perkin Elmer SPCM-AQR-16 - Single Photon Counting Module

Thorlabs S 132A - Germanium Power Sensor 700-1800nm (to measure average powers)

EO Tech ET 3500F - InGaAs PIN Detector (to measure the laser rep rate)

A.2 Optical Elements

Newport 5721-A-H - Aspheric Lens 2.8mm focal length

Thorlabs BP145B3 - Pellicle Beam Splitter 45:55 R:T for 1μm - 2μm

Thorlabs NDC-50C-2M - Variable OD Filter Wheel

Thorlabs PF10-03-M01 - Gold Mirrors 800nm - 20μm **Thorlabs LJ-1277L1-C** - Cylindrical lens 250mm focal length **Thorlabs LJ-1821L1-C** - Cylindrical lens 50.8mm focal length

A.3 Sources

Fiber Laser - Lab Built Fiber Laser at 38MHz

Spectra Diode Labs SDL 800 - Amplifier Diode Driver

A.4 Autocorrelation Setup

LabWorks Inc. pa-119 - Linear Power Amplifier (controls the shaker oscillation amplitude)

Hewlett Packard 33120A - Function Generator to drive the shaker

Brüel and Kjær 4810 Electromagnetic Shaker

A.5 Measurement

Agilent 86142B - Optical Spectrum Analyser

Stanford Research Systems SR570 - Low Noise Current Preamplifier

Tektronix TDS 2012C - Oscilloscope

BK Precision 1823A - Universal Frequency Counter (to count photons from the SPCM)

National Instruments BNC-2121 - Faster Frequency Counter (to count photons from the SPCM)

APPENDIX B

IMAGE SOURCES

Fig. 2.1 [6]

Fig. 2.2 [3]

Fig. 2.3 Self

Fig. 2.4 Self

Fig. 2.5 Self

Fig. 3.1 Hamamatsu S-1223-01 Datasheet

Fig. 3.2 Self Measured

Fig. 3.3 Self Measured

Fig. 3.4 Self

Fig. 3.5 Self Measured

Fig. 4.1 Self Measured

Fig. 4.2 Self

Fig. 4.3 Self Measured

Fig. 4.4 Self Measured

Fig. 4.5 Self Measured

Fig. 4.6 Self Measured

Fig. 4.7 Self Measured

Fig. 5.1 Measured by Kasturi Saha

Fig. 5.2 Self

BIBLIOGRAPHY

[1] Patrick Gill. Optical frequency standards. *Metrologia*, 42(3):S125–S137, June 2005.

[2] CW Chou, DB Hume, T. Rosenband, and DJ Wineland. Optical clocks and relativity. *Science*, (September):4–7, 2010.

[3] Jun Ye and ST Cundiff. *Femtosecond optical frequency comb: Principle, Operation and Applications*. Springer, 2004.

[4] R Holzwarth, T Udem, Tw Hansch, Jc Knight, Wj Wadsworth, and Ps Russell. Optical frequency synthesizer for precision spectroscopy. *Physical Review Letters*, 85(11):2264–7, September 2000.

[5] Christoph Gohle, Thomas Udem, Maximilian Herrmann, Jens Rauschenberger, Ronald Holzwarth, Hans a Schuessler, Ferenc Krausz, and Theodor W Hänsch. A frequency comb in the extreme ultraviolet. *Nature*, 436(7048):234–7, July 2005.

[6] T J Kippenberg, R Holzwarth, and S a Diddams. Microresonator-based optical frequency combs. *Science*, 332(6029):555–9, April 2011.

[7] D E Spence, P N Kean, and W Sibbett. 60-fsec pulse generation from a self-mode-locked Ti:sapphire laser. *Optics letters*, 16(1):42–4, January 1991.

[8] A. Bartels, T. Dekorsy, and H. Kurz. Unidirectionally modelocked fs Ti:sapphire ring laser with 1 GHz repetition rate and its application in spectroscopy. In *Technical Digest. Summaries of papers presented at the Conference on Lasers and Electro-Optics. Postconference Edition. CLEO '99. Conference on Lasers and Electro-Optics (IEEE Cat. No.99CH37013)*, page 60. Opt. Soc. America.

[9] Verena Mackowiak, Phillip Kubina, Peter Adel, Ronald Holzwarth, and Theodor W. Hänsch. Advances in Ti:Sapphire and Er Fiber Based Femtosecond Laser Frequency Comb Systems - Technical Digest (CD). In *Conference on Lasers and Electro-Optics/Quantum Electronics and Laser Science and Photonic Applications Systems Technologies*, page JWB6. Optical Society of America, May 2005.

[10] P Del'Haye, A Schliesser, O Arcizet, T Wilken, R Holzwarth, and T J Kip-

penberg. Optical frequency comb generation from a monolithic microresonator. *Nature*, 450(7173):1214–7, December 2007.

[11] Imad H. Agha, Yoshitomo Okawachi, and Alexander L. Gaeta. Theoretical and experimental investigation of broadband cascaded four-wave mixing in high-Q microspheres. *Optics Express*, 17(18):16209, August 2009.

[12] Anatoliy Savchenkov, Andrey Matsko, Vladimir Ilchenko, Iouri Solomatine, David Seidel, and Lute Maleki. Tunable Optical Frequency Comb with a Crystalline Whispering Gallery Mode Resonator. *Physical Review Letters*, 101(9):093902, August 2008.

[13] Yoshitomo Okawachi, Kasturi Saha, Jacob S Levy, Y Henry Wen, Michal Lipson, and Alexander L Gaeta. Octave-spanning frequency comb generation in a silicon nitride chip. *Optics Letters*, 36(17):3398–400, September 2011.

[14] Rick Trebino. Measuring the seemingly immeasurable. *Nature Photonics*, 5(April):189–192, 2011.

[15] H. P. Weber. Method for Pulsewidth Measurement of Ultrashort Light Pulses Generated by Phase-Locked Lasers using Nonlinear Optics. *Journal of Applied Physics*, 38(5):2231, 1967.

[16] M Maier, W Kaiser, and JA Giordmaine. Intense Light Bursts in the stimulated Raman effect. *Physical Review Letters*, (2):1275–1277, 1966.

[17] Rick Trebino, Selcuk Akturk, Steven T Cundiff, Franz X Kaertner, and Joshua Et al. *Ultrafast Optics Textbook*. Unpublished, 2013.

[18] Robert W Boyd. *Nonlinear Optics*. Academic Press, 3rd edition, 2008.

[19] Jean-Claude Diels and Wolfgang Rudolph. *Ultrashort Laser Pulse Phenomena : Fundamentals, Techniques, and Applications on a Femtosecond Time Scale*. Academic Press, 2nd edition, 2006.

[20] Reza Salem. *Characterisation Of Two-Photon Absorption Detectors For Applications In High-Speed Optical Systems*. Masters thesis, University of Maryland, 2003.

[21] C. Xu, J.M. Roth, W.H. Knox, and K. Bergman. Ultra-sensitive autocorrela-

tion of 1.5μm light with single photon counting silicon avalanche photodiode. *Electronics Letters*, 38(2):86, 2002.

[22] Eugene Hecht. *Optics*. Pearson Education Inc., 4th edition, 2002.